ATLAS NOTE

CONF-SUSY-2015-02

20th March 2015

Combination of searches for strongly-produced supersymmetric particles with the ATLAS detector in proton–proton collisions at $\sqrt{s} = 8$ TeV

The ATLAS Collaboration

Abstract

This note presents the combination of three ATLAS searches for squarks and gluinos in 20 fb^{-1} of proton–proton collisions at $\sqrt{s} = 8$ TeV. The results of searches in final states with jets, missing transverse momentum and no or one isolated lepton are combined and interpreted in two simplified models where pair-produced squarks or gluinos decay through an intermediate chargino to the lightest stable supersymmetrical particle. In the model of pair-produced gluinos, gluinos below 1.3 TeV are excluded at 95% CL, for a neutralino mass below 500 GeV. Squarks are excluded in a similar model up to 850 GeV at 95% CL for massless neutralinos. These limits are an improvement of approximately 50 GeV with respect to the results of the separate analyses.

ATLAS-CONF-2015-011
20 March 2015

1. Introduction

Many extensions of the Standard Model (SM) include heavy coloured particles. Some of these could be accessible at the Large Hadron Collider (LHC) [1], including for example squarks ($\tilde{q}$) and gluinos ($\tilde{g}$) of supersymmetric (SUSY) theories [2–10]. In SUSY theories squarks $\tilde{q}_{\mathrm{L}}$ and $\tilde{q}_{\mathrm{R}}$ are the partners of the left- and right-handed SM quarks, respectively, and gluinos ($\tilde{g}$) are the partners of the SM gluons. The partners of the neutral and charged SM gauge and Higgs bosons are the neutralinos ($\tilde{\chi}^0$) and charginos ($\tilde{\chi}^{\pm}$), respectively.

This note presents a combination of searches for squarks and gluinos in final states containing jets with high transverse momentum (p_{T}), possibly leptons, and large missing transverse momentum ($E_{\mathrm{T}}^{\mathrm{miss}}$). Interest in these final states is motivated by the large number of R-parity-conserving [11–15] SUSY models in which squarks and gluinos can be produced in pairs ($\tilde{g}\tilde{g}$, $\tilde{q}\tilde{q}$, $\tilde{q}\tilde{g}$; no distinction is made between squarks and anti-squarks) and can decay through $\tilde{q} \rightarrow q'\tilde{\chi}^{\pm}$ (where $\tilde{q}$ and q' are of different flavour) and $\tilde{g} \rightarrow q'\bar{q}\tilde{\chi}^{\pm}$ (where $\bar{q}$ and q' are of different flavour). These charginos subsequently decay to $W^{\pm}\tilde{\chi}_1^0$, where $\tilde{\chi}_1^0$ is the lightest SUSY particle (LSP) in these models. Being neutral, weakly interacting and stable, the $\tilde{\chi}_1^0$ escapes the detector without being detected and thus results in missing transverse momentum. These processes are illustrated in Fig. 1. Simplified models of direct decays $\tilde{q} \rightarrow q\tilde{\chi}_1^0$ and $\tilde{g} \rightarrow qq'\tilde{\chi}_1^0$ are not used in this work, as the sensitivity to them does not benefit from a combination.

A combination of three different SUSY analyses searching for squark and gluino production in final states with or without leptons is presented. The analysis studying final states with jets, missing transverse momentum and no leptons, referred to as the *0-lepton analysis*, was reported in Ref. [16]. The other two analyses requiring either a low or a high p_{T} electron or muon were reported in Ref. [17] and are referred to as the *1-lepton analyses*.

The three analyses interpreted their results in multiple SUSY models. In several of these models, the 0-lepton and the 1-lepton analyses have similar sensitivities. As a consequence, a combination of the three analyses is expected to result in an increase in sensitivity.

After a brief description of the ATLAS detector in Section 2, a summary of the 0-lepton and 1-lepton analyses is given in Section 3. The combination procedure is explained in Section 4, with a specific discussion of the correlated systematic uncertainties. The results of the combination are presented in Section 5.

2. ATLAS detector

ATLAS [18] is a multipurpose particle physics detector with a forward-backward symmetric cylindrical geometry and nearly 4π coverage in solid angle.[1] The layout of the detector is dominated by four superconducting magnet systems, which comprise a thin solenoid surrounding inner tracking detectors (ID) with $|\eta| < 2.5$ and three large toroids supporting a large muon spectrometer (MS). The MS covers a range of $|\eta| < 2.7$ for precision measurements and $|\eta| < 2.4$ for triggering purposes. In the pseudorapidity

[1] ATLAS uses a right-handed coordinate system with its origin at the nominal interaction point in the centre of the detector and the z-axis along the beam pipe. Cylindrical coordinates (r, ϕ) are used in the transverse plane, ϕ being the azimuthal angle around the beam direction. The pseudorapidity η is defined in terms of the polar angle θ by $\eta = -\ln\tan(\theta/2)$.

region $|\eta| < 3.2$, high-granularity liquid-argon (LAr) electromagnetic (EM) sampling calorimeters surround the solenoid magnet. A steel-scintillator tile calorimeter provides hadronic coverage over $|\eta| < 1.7$. The end-cap and forward regions, spanning $1.5 < |\eta| < 4.9$, are instrumented with LAr calorimeters for both EM and hadronic measurements.

3. Analysis overview

The 0-lepton and 1-lepton analyses select events with high-momentum jets and large missing transverse momentum. They are statistically independent due to a veto on any electron or muon with $p_{\mathrm{T}} > 10$ GeV in the former case and requiring an electron or muon with $p_{\mathrm{T}}(e/\mu) > 25$ GeV (hard 1-lepton) or $p_{\mathrm{T}}(e/\mu) > 7/6$ GeV (soft 1-lepton) in the latter. It has been checked explicitly that the difference in lepton-p_{T} thresholds in the 0-lepton and soft 1-lepton analyses result in no overlapping events. The three analyses can therefore be combined. In the following, the signal models targeted and the events selected are briefly described.

3.1. Supersymmetry models

This note specifically discusses a simplified model [19] in which pair-produced squarks or gluinos decay through an intermediate chargino to the LSP. Diagrams for both decays are shown in Figure 1. The mass of the chargino is chosen to lie between the squark or gluino mass and the LSP mass and is determined by $x = \frac{m(\tilde{\chi}^{\pm}) - m(\tilde{\chi}_1^0)}{m(\tilde{q},\tilde{g}) - m(\tilde{\chi}_1^0)} = \frac{1}{2}$. A branching ratio of 100% is assumed for $\tilde{q} \to q\tilde{\chi}_1^{\pm} \to qW\tilde{\chi}_1^0$ decays and $\tilde{g} \to q\bar{q}\tilde{\chi}_1^{\pm} \to q\bar{q}W\tilde{\chi}_1^0$ decays. All other sparticles are decoupled by treating them as very heavy.

Signal events are generated with up to one additional parton in the matrix element, using MadGraph5 1.5.4 interfaced to pythia-6.426. More details about the signal simulation samples can be found in [16, 17].

3.2. Event selections

Two sets of signal and control regions are used in the analyses, which are extensively documented in the respective papers. They are briefly summarised here.

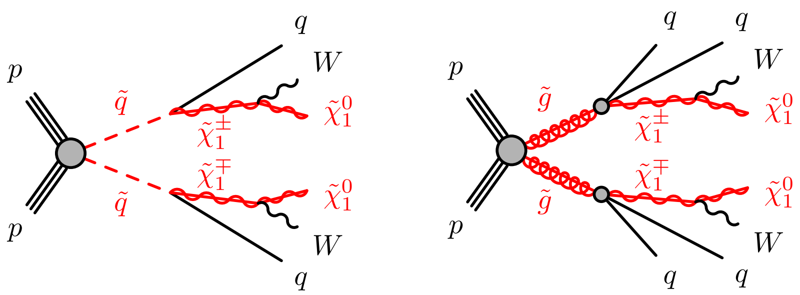

Figure 1: The decay topologies of squark-pair production (left) and gluino-pair production (right), in simplified models with decays of squarks and gluinos via an intermediate chargino.

The 0-lepton analysis selects events with at least 2 to 6 jets with $p_T > 130$ GeV for the leading jet and $p_T > 60$ GeV for any further selected jet, and $E_T^{miss} > 160$ GeV. Events are required to not contain any electron or muon with $p_T > 10$ GeV. In total, 15 partly overlapping signal regions are defined that select events based on the effective mass $m_{eff} = \sum_i |p_T^i| + E_T^{miss}$, where the sum runs over all jets with $p_T > 40$ GeV in the event, and the ratio $E_T^{miss}/m_{eff}(N_j)$, where the sum over jet p_T in the definition of $m_{eff}(N_j)$ only includes jets with $p_T > 60$ GeV. Major backgrounds are estimated using dedicated control regions that are enriched in W+jets, $t\bar{t}$ and single-top, Z+jets or multijets background events. The W and Top control regions, which require a high p_T electron or muon, have been slightly modified with respect to the original regions used in [16]. Events that are selected by the respective W and Top control regions in the 1-lepton analyses are vetoed. This modification is necessary to ensure a complete statistical independence of the three analyses. The sensitivity of the 0-lepton analysis is not affected by this modification of the control regions.

The 1-lepton analyses require events with at least one electron or muon in the final state. Based on the p_T of the lepton, the event is categorised as hard ($p_T(e/\mu) > 25$ GeV) or soft ($7/6 < p_T(e/\mu) < 25$ GeV). Both sets of events are further categorised according to the number of jets, the p_T of those jets, E_T^{miss}, the transverse mass $m_T = \sqrt{2 p_T^{\ell} E_T^{miss}(1 - \cos[\Delta\phi(\vec{\ell}, \boldsymbol{E}_T^{miss})])}$, and m_{eff}. The definition of the effective mass also includes the lepton p_T in the case of the 1-lepton analyses. The soft 1-lepton analysis uses two different signal regions with different jet multiplicities, or one inclusive signal region if it performs better than the other two. The hard 1-lepton analysis uses three different signal regions with different jet multiplicities, ranging from at least three to at least six jets. As all the soft and hard 1-lepton signal regions are statistically independent, they are always used in the combination.

4. Combination procedure

The result is obtained by combining the individual likelihoods of the 0-lepton and 1-lepton analyses. In the case of the 0-lepton analysis the likelihood for the signal region that provides the best expected CL_s value [20] for the signal model considered, and its corresponding control regions, is chosen. The choice of signal region can vary as a function of sparticle mass. For the 1-lepton analyses, all the available signal regions are orthogonal. A single likelihood that describes all of them serves as input for the combination procedure. Some of the systematic uncertainties can be correlated when building the combined likelihood. The correlated uncertainties in the combination procedure are the luminosity uncertainty, the uncertainty on the SUSY cross-section, b-tagging uncertainties, the jet energy resolution and E_T^{miss}-related uncertainties. Other systematic uncertainties, such as theoretical uncertainties, could not be correlated, e.g. those due to different Monte Carlo generators used in the 0-lepton and 1-lepton analyses. The jet energy scale uncertainty is not correlated, due to the use of different prescriptions in the analyses. A profile likelihood fit is performed using HistFitter [21] to obtain the results.

The combination of the analyses was carefully validated by ensuring that the combined likelihood did not lead to artificial correlations between fit parameters or major changes in post-fit values of nuisance parameters with respect to the results discussed in Refs.[16, 17].

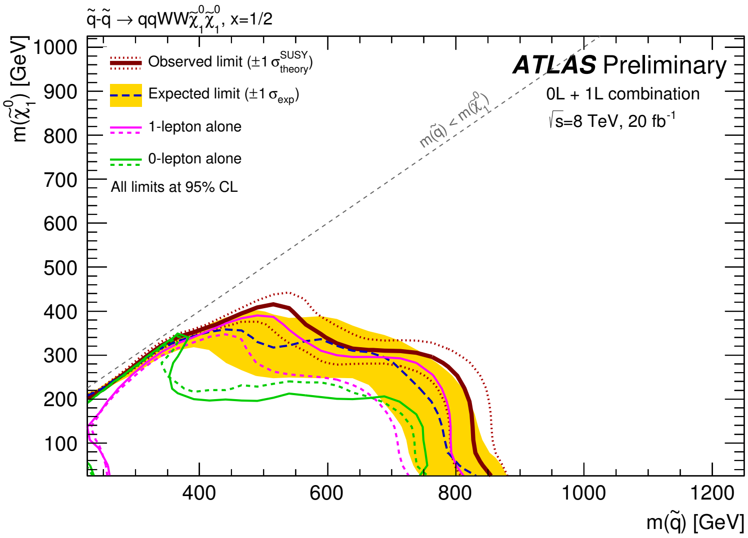

Figure 2: Observed and expected limits for simplified models of squark-pair production with decays through an intermediate chargino, for chargino masses exactly half the mass difference between the squark mass and the LSP mass. The yellow band includes all experimental uncertainties; the red dotted lines indicate the theory uncertainty on the cross-section. The individual limits from the 0-lepton analysis [16] and the 1-lepton analyses [17] are overlaid in green and magenta, respectively.

5. Results

Figures 2 and 3 show the result of the combination of the three analyses for both squark-pair and gluino-pair production. The limits obtained improve the results of the separate analyses significantly, reaching higher $\tilde{\chi}_1^0$ mass and approximately 50 GeV higher squark or gluino mass for massless neutralinos. The combined limit also approaches the diagonal $m(\tilde{\chi}_1^0) = m(\tilde{q}, \tilde{g})$ closer than either of the individual analyses on its own.

6. Summary

In this note, a statistical combination of three published analyses searching for squark- and gluino-pair production with final states involving jets, missing transverse momentum and either no electron or muon, one low p_{T} or one high p_{T} electron or muon was presented.

Limits were calculated in two simplified models of squark- and gluino-pair production in which the squarks and gluinos decay via intermediate charginos. When the sensitivities of the individual analyses are similar, the combination increases the overall sensitivity. Most notably, the limits in the model of gluino-pair production extend up to $m(\tilde{g}) \sim 1.3$ TeV for low $\tilde{\chi}_1^0$ masses, improving the sensitivities of the individual analyses by approximately 50 GeV.

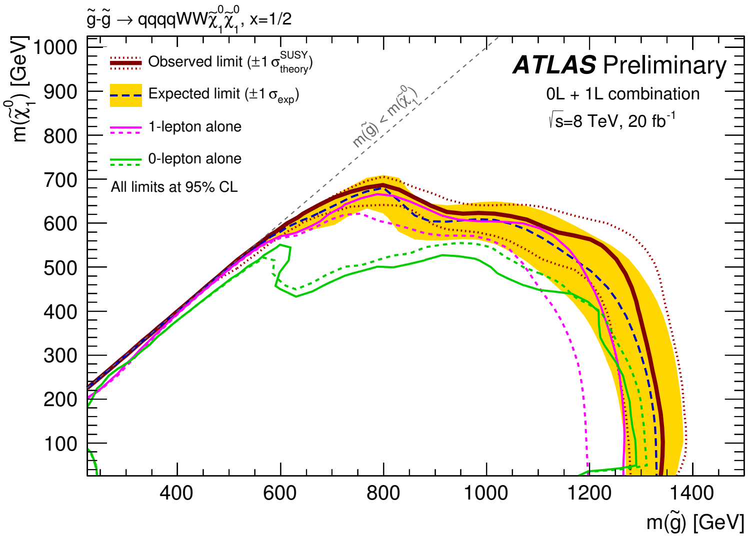

Figure 3: Observed and expected limits for simplified models of gluino-pair production with decays through an intermediate chargino, for chargino masses exactly half the mass difference between the gluino mass and the LSP mass. The yellow band includes all experimental uncertainties; the red dotted lines indicate the theory uncertainty on the cross-section. The individual limits from the 0-lepton analysis [16] and the 1-lepton analyses [17] are overlaid in green and magenta, respectively.

References

[1] L. Evans and P. Bryant, *LHC Machine*, JINST **3** (2008) S08001.

[2] H. Miyazawa, *Baryon Number Changing Currents*, *Prog. Theor. Phys.* **36 (6)** (1966) 1266–1276.

[3] P. Ramond, *Dual Theory for Free Fermions*, *Phys. Rev.* **D 3** (1971) 2415–2418.

[4] Y. A. Golfand and E. P. Likhtman, *Extension of the Algebra of Poincare Group Generators and Violation of p Invariance*, JETP Lett. **13** (1971) 323–326, [Pisma Zh. Eksp. Teor. Fiz. 13 (1971) 452-455].

[5] A. Neveu and J. H. Schwarz, *Factorizable dual model of pions*, *Nucl. Phys.* **B 31** (1971) 86–112.

[6] A. Neveu and J. H. Schwarz, *Quark Model of Dual Pions*, *Phys. Rev.* **D 4** (1971) 1109–1111.

[7] J. Gervais and B. Sakita, *Field theory interpretation of supergauges in dual models*, *Nucl. Phys.* **B 34** (1971) 632–639.

[8] D. V. Volkov and V. P. Akulov, *Is the Neutrino a Goldstone Particle?*, *Phys. Lett.* **B 46** (1973) 109–110.

[9] J. Wess and B. Zumino, *A Lagrangian Model Invariant Under Supergauge Transformations*, *Phys. Lett.* **B 49** (1974) 52.

[10] J. Wess and B. Zumino, *Supergauge Transformations in Four-Dimensions*, *Nucl. Phys.* **B 70** (1974) 39–50.

[11] P. Fayet, *Supersymmetry and Weak, Electromagnetic and Strong Interactions*, *Phys. Lett.* **B 64** (1976) 159.

[12] P. Fayet, *Spontaneously Broken Supersymmetric Theories of Weak, Electromagnetic and Strong Interactions*, *Phys. Lett.* **B 69** (1977) 489.

[13] G. R. Farrar and P. Fayet, *Phenomenology of the Production, Decay, and Detection of New Hadronic States Associated with Supersymmetry*, *Phys. Lett.* **B 76** (1978) 575–579.

[14] P. Fayet, *Relations Between the Masses of the Superpartners of Leptons and Quarks, the Goldstino Couplings and the Neutral Currents*, *Phys. Lett.* **B 84** (1979) 416.

[15] S. Dimopoulos and H. Georgi, *Softly Broken Supersymmetry and SU(5)*, *Nucl. Phys.* **B 193** (1981) 150.

[16] ATLAS Collaboration, *Search for squarks and gluinos with the ATLAS detector in final states with jets and missing transverse momentum using* $\sqrt{s} = 8$ *TeV proton–proton collision data*, JHEP **1409** (2014) 176, arXiv: `1405.7875 [hep-ex]`.

[17] ATLAS Collaboration, *Search for squarks and gluinos in events with isolated leptons, jets and missing transverse momentum at* $\sqrt{s} = 8$ *TeV with the ATLAS detector* (2015), arXiv: `1501.03555 [hep-ex]`.

[18] ATLAS Collaboration, *The ATLAS Experiment at the CERN Large Hadron Collider*, JINST **3** (2008) S08003.

[19] C. Gutschow and Z. Marshall, *Setting limits on supersymmetry using simplified models* (2012), arXiv: `1202.2662 [hep-ex]`.

[20] A. Read, *Presentation of search results: the CLs technique*, Journal of Physics G: Nucl. Part. Phys. **28** (2002) 2693–2704.

[21] M. Baak et al., *HistFitter software framework for statistical data analysis* (2014), arXiv: `1410.1280 [hep-ex]`.

A. Auxiliary figures

Figs. 4 and 5 show the result without lines indicating the theory uncertainty on the cross-section.

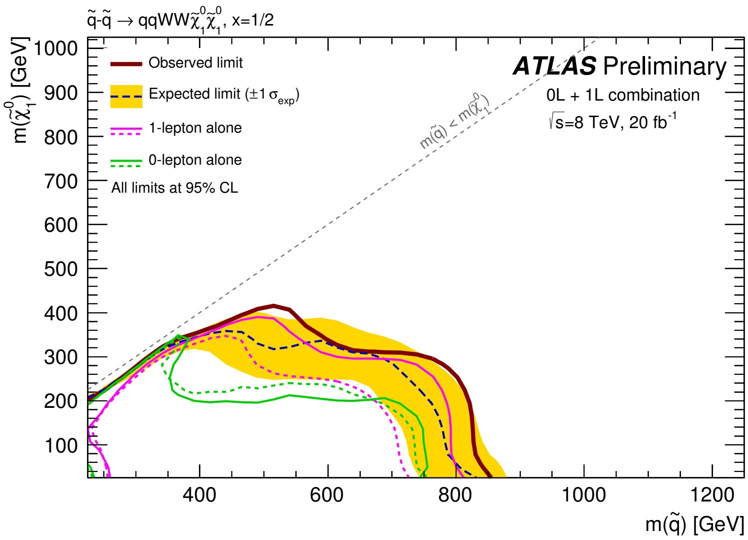

Figure 4: Observed and expected limits for simplified models of squark-pair production with decays through an intermediate chargino, for chargino masses exactly half the mass difference between the squark mass and the LSP mass. The yellow band includes all experimental uncertainties. The individual limits from the 0-lepton analysis [16] and the 1-lepton analyses [17] are overlaid in green and magenta, respectively.

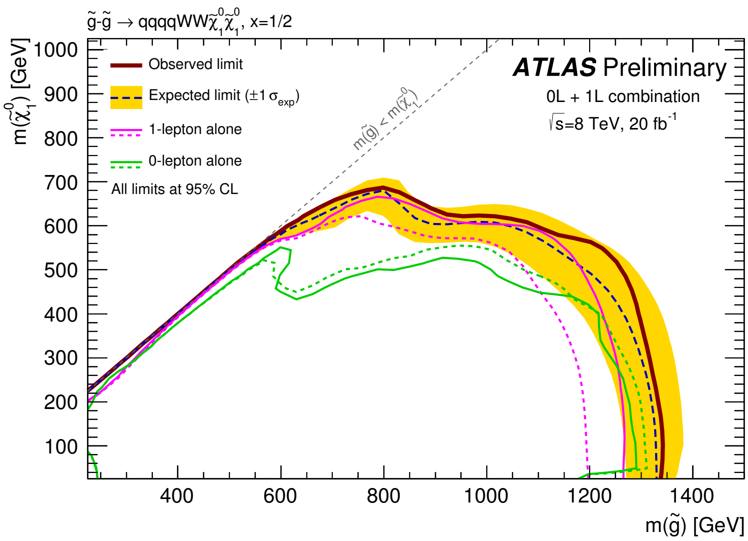

Figure 5: Observed and expected limits for simplified models of gluino-pair production with decays through an intermediate chargino, for chargino masses exactly half the mass difference between the gluino mass and the LSP mass. The yellow band includes all experimental uncertainties. The individual limits from the 0-lepton analysis [16] and the 1-lepton analyses [17] are overlaid in green and magenta, respectively.